Pathology - Research and Practice 215 (2019) 152574

Contents lists available at ScienceDirect

Pathology - Research and Practice

journal homepage: www.elsevier.com/locate/prp

Size distribution of serum extracellular vesicles in mice with atherosclerosis

Seokmin Kang[e,1], Jung Wook Yang[d,1], Joo Yeon Jeong[b], Juyeong Park[b], Hyo Jung An[a], Hyun Min Koh[a], Se Min Jang[a], Yoon Jung Lee[c], Dae Hyun Song[a,b,c,*]

[a] Department of Pathology, Gyeongsang National University Changwon Hospital, Changwon, Republic of Korea
[b] Gyeongsang National University School of Medicine, Jinju, Republic of Korea
[c] Gyeongsang Institute of Health Science, Jinju, Republic of Korea
[d] Department of Pathology, Gyeongsang National University Hospital, Jinju, Republic of Korea
[e] Korea Brain Research Institute, Daegu, Republic of Korea

ARTICLE INFO

Keywords:
Atherosclerosis
Aorta
Heart
Extracellular vesicles
Mouse

ABSTRACT

Background and aims: Atherosclerosis is a prominent vascular lesion, and potentially causing ischemic alterations in the brain and heart. Recent studies have reported that physiological and pathological alterations in atherosclerosis and extracellular vesicles (EV) are related. This study aimed to investigate the association between the extent of atherosclerotic lesions and the number of serum EVs in a mouse model of atherosclerosis (*wild-type*).

Methods: Eighteen 3-week-old C57BL/6 N male mice(*wild-type*) were purchased. Twelve mice were fed a 45% high-fat diet (HFD) for six months. Six mice were provided standard laboratory chow for six months. The entire aorta, from the aortic sinus to the division of the iliac artery, was dissected out from each mouse. Furthermore, the degree of atherosclerosis was microscopically determined. Serum EVs were quantified by size via nanoparticle tracking analysis.

Results: The number of EVs in the high-atherosclerotic score group (1.43×10^9) was higher than that in the low-atherosclerotic score group (0.7×10^9) in the range of 211.5–222.5 nm ($p = 0.033$).

Conclusions: Enumeration of EVs is a potential method of detecting atherosclerosis.

1. Introduction

Atherosclerosis is a prominent vascular lesion, causing fatal diseases, and it can cause ischemic alterations in the brain and heart [6]. Recent studies have reported associations between physiological and pathological changes in atherosclerosis and extracellular vesicles (EV) [2,4,5,8,12]. EVs were analysed as two aspects, those are quantitative analysis and qualitative analysis. The qualification means the biomolecular contents in EVs which can work as material with cell to cell communication. The quantification of EVs is also important to use as biomarker with concept of liquid biopsy. Perrotta et al. reported that increased number of microvesicular bodies which is the precursors of exosomes is observed in electron microscopic study of atherosclerotic lesions [5]. In this study, we investigated the association between the extent of atherosclerotic lesions and the number of serum EVs in a mouse model of atherosclerosis (*wild-type*).

2. Materials and methods

2.1. Animal model

Eighteen 3-week-old C57BL/6N male mice(*wild-type*) were purchased from Koatech(Pyeongtaek, South Korea, http://www.koatech.co.kr/). The mice were randomly divided into two groups. Twelve mice were fed a 45% high-fat diet (HFD) for six months, and six mice were fed standard laboratory chow for six months. The mice were housed in a sanitized animal laboratory and weighed every week. The date of euthanasia was decided on the basis of differences in body weight (Fig. 1). All protocols were approved by the Gyeongsang National University Institutional Animal Care and Use Committee (GNU-170905-M0042).

2.2. Obtainment of aortic specimens

After six months of feeding, mice were euthanized. Thereafter, whole blood samples were maximally collected via cardiac puncture.

* Corresponding author at: Department of Pathology, Gyeongsang National, University School of Medicine, 79 Gangnam-ro, Jinju 52727, Republic of Korea.
E-mail address: golgy@hanmail.net (D.H. Song).
[1] Seokmin Kang and Jung Wook Yang have contributed equally as first authors.

https://doi.org/10.1016/j.prp.2019.152574
Received 29 May 2019; Received in revised form 15 July 2019; Accepted 31 July 2019

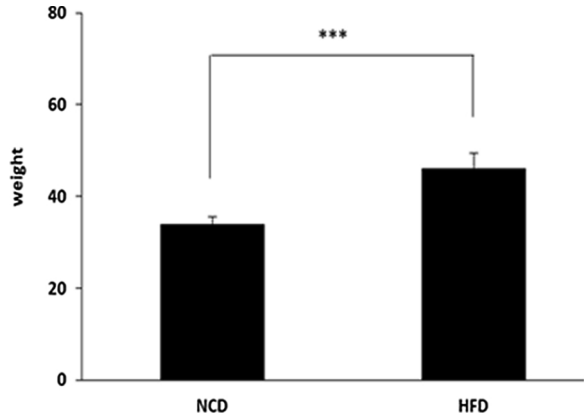

Fig. 1. Differentiation of body weight between the NCD group and HFD group. NCD, normal chewing diet; HFD, high fat diet.
***P < 0.001.

The aorta was cleaned via perfusion with PBS and fixed with 10% glutaraldehyde. Thereafter, the entire aorta, from the aortic sinus to the division of the iliac artery, was dissected out from each mouse. Fully progressed fatty liver which is almost 100% of proportion could be observed at all high fat diet mice in gross observation.

2.3. Oil red O staining of frozen sections

Aortic specimens were grossly examined and divided into three parts, each from aortic sinus (AS), aortic arch (AR), and aorta containing the descending thoracic aorta and abdominal aorta (AT). Each part was serially dissected at 0.5 cm intervals. All specimens were frozen for Oil red O staining. Frozen tissue, embedded in Surgipath FSC 2 clear frozen section compound (Richmond, IL, USA, Leica Biosystems), was cut into 8-μm samples and placed on the glass slide. To minimize sample loss, the glass slide was dried on a 52 ˚C heat block and then carefully washed in distilled water for one minute to eliminate the frozen section compound material. At room temperature (27 ℃), Oil red O staining was performed for 5 min with a mixture of 0.7 g Oil red O (Saint Louis, USA, Sigma-Aldrich, cat.O0625) and 100 ml propylene glycol, and heated up to 100℃ and filtered. After cleaning with distilled water, it was gently immersed in 70% ethyl alcohol (EtOH) thrice and then in 90% EtOH once. Further washing was carried out microscopically to prevent overstaining. After staining with hematoxylin for 1 min, the specimens were washed with distilled water. After microscopic observation, additional cleaning was performed with80% EtOH and distilled water. Specimens were mounted in glycerin. To exclude false-positive signals, the aortic endovascular lumen was considered the negative control. Positive signals in the aortic vascular wall, accompanied by histologic changes including wall thickening or cleft formation in the vascular wall were considered true signals (Fig. 2). All tests were repeatedly conducted more than three times to prevent tissue loss.

2.4. Quantification of atherosclerotic lesions

All sections of AS, AR, and AT were carefully evaluated for the number of aortic tissue sections (section N),the number of aortic tissue sections with atherosclerosis(section score), the proportion of atherosclerotic lesions at each section(proportion score), and the calculated score of atherosclerosis in each part(total score). The atherosclerosis score(Ats) of each mouse was measured by adding up the total scores of AS, AR, and AT (Table 1).

2.5. Quantification of serum EVs

Mouse blood samples were collected and centrifuged (3000 rpm, 10 min, 4℃) to collect serum. Supernatant serum fraction was centrifuged (2000 × *g*, 10 min, 4℃) to remove any cell and cellular debris. The supernatants were filtered through a 0.22-μm filter(Acrodisc 25 mm syringe filter, PALL Life sciences, Ann Arbor, MI, USA) and

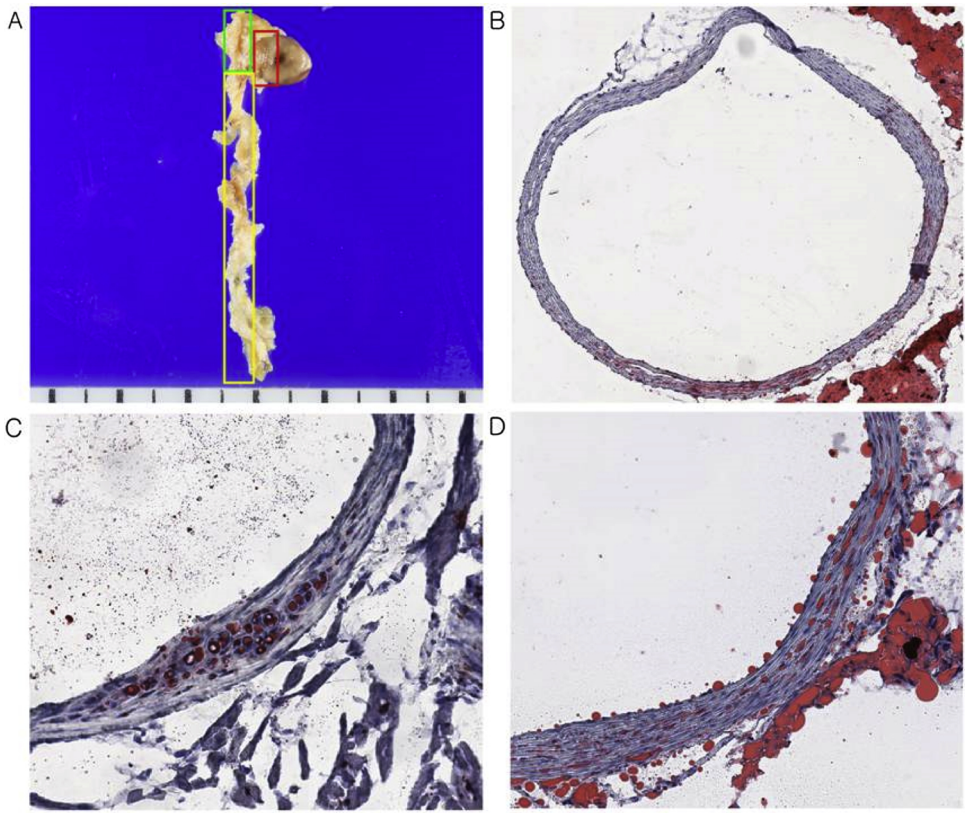

Fig. 2. Atheroslcerotic lesion in aorta of the mice.
A) The aortic sample was grossly examined and devided into three parts, each from aortic sinus (AS, red), aortic arch (AR, green) and aorta contains descending thoracic aorta and abdominal aorta (AT, yellow). B) There is an area of positive signals (right lower) in vascular wall. The internal lumen shows negative signal (negative control) and perivascular fatty tissue exhibits positive signal (positive control)[original magnification x40, oil red O stain]. C) The atherosclerotic lesion in aortic sinus exhibits positive signal with thickening of wall [original magnification x100, oil red O stain]. D) Red droplets (positive signal) detects lipid components of atherosclerotic lesion of vascular wall with cleft [original magnification x100, oil red O stain].

Table 1
Atherosclerotic scores of 18 mice.

Group	Wt. (g)	AS				AR				AT				Ats	EVs (211.5˜222.5 nm)	EVs of Low Ats (less than 0.5) vs. EVs of High Ats (not less than 0.5)
		N	SS	PS	TS	N	SS	PS	TS	N	SS	PS	TS			
NCD1	34.69	0	0	0	0	0	0	0	0	1	0	0	0	0	IA	P = 0.033
NCD2	34.96	1	0	0	0	1	0	0	0	5	1	0.05	0.01	0.01	2452477000	
NCD3	31.81	1	0	0	0	1	0	0	0	5	0	0	0	0	2018549750	
NCD4	33.92	1	0	0	0	1	0	0	0	5	0	0	0	0	3472352750	
NCD5	36.02	0	0	0	0	1	1	0.2	0.2	6	0	0	0	0.2	598794000	
NCD6	32.21	1	0	0	0	1	1	0.2	0.2	3	0	0	0	0.2	IA	
HFD1	49.98	1	0	0	0	1	1	0.2	0.2	4	0	0	0	0.2	1356317360	Low Ats
HFD2	44.76	1	0	0	0	1	1	0.75	0.75	3	0	0	0	0.75	986023960	High Ats
HFD3	41.13	1	0	0	0	1	1	0.3	0.3	5	0	0	0	0.3	321922440	Low Ats
HFD4	44.59	1	0	0	0	1	1	0.9	0.9	4	0	0	0	0.9	231704960	High Ats
HFD5	42.14	1	1	0.15	0.15	2	1	0.8	0.4	2	0	0	0	0.55	2011182200	High Ats
HFD6	46.46	1	1	0.1	0.1	2	1	0.5	0.25	3	2	0.1/0.15	0.08	0.43	196474600	Low Ats
HFD7	50.59	1	0	0	0	1	1	0.7	0.7	3	0	0	0	0.7	2185315480	High Ats
HFD8	47.67	1	0	0	0	2	2	0.5/0.3	0.4	2	0	0	0	0.4	797915920	Low Ats
HFD9	47.1	1	1	0.1	0.1	2	0	0	0	4	0	0	0	0.1	585717360	Low Ats
HFD10	48.76	0	0	0	0	1	1	0.1	0.1	1	0	0	0	0.1	672145400	Low Ats
HFD11	42.37	1	1	0.05	0.05	1	1	0.75	0.75	3	0	0	0	0.8	1749625960	High Ats
HFD12	49.07	1	0	0	0	2	2	0.5/0.15	0.33	3	0	0	0	0.33	1036733000	Low Ats

Wt., body weight; AS, aortic sinus; AR, aortic arch; AT, descending thoracic aorta to abdominal aorta; Ats, atherosclerotic score; N, number of the aortic section (section N); SS, section score; PS, proportion score; TS, total score; NCD, normal chewing diet; HFD, high fat diet; EVs, The number of extracellular vesicles at 100 ul of serum; IA, inadequate specimen; *Total score* $= \frac{\sum_1^n \text{section score*proportion score}}{\text{section N}}$, Ats score= TS of AS+ TS of AR+ TS of AT.

ultracentrifuged at 120,000 $\times g$ for 90 min(4℃). The pellet was washed with PBS and ultracentrifuged at 120,000 $\times g$ for 90 min (4℃). After eliminating the supernatant, the pellet was resuspended 100 μl particle-free PBS and prepared for subsequent analysis [10,11].

The EV size distribution and concentration were determined using a NanoSight LM10 nanoparticle tracking analysis(NTA) system(Malvern Ins., Malvern, UK) as described previously [3]. The eluate was used for NTA with 100 μl of filtered Dulbecco's Phosphate-Buffered Saline (DPBS), followed by evaluation using the NTA software(version 2.1)

3. Results

3.1. Identification of atherosclerotic lesions in aortic tissue

After the six-month experiment, the average weight of the HFD group was 46.22 g and that of the control group was 33.93 g, displaying a significant difference in weight ($p < 0.001$) (Fig. 1). An average of one tissue section was obtained in AS, and 4 of 12 HFD group contained atherosclerotic lesions, with the proportion of the total vascular wall being approximately 10%. In the normal chewing diet(NCD) group, no atherosclerotic lesions were observed in the AS specimens (Table 1). In almost every mouse in the NCD and HFD group, more than one piece of AR tissue was observed, and tissue fragments displayed up to 90% lesions in the HFD. The section score for AT was higher than that of other parts but not the proportion score (Table 1). Weight was not significantly associated with the Ats($p = 0.054$). All high-Ats(more than 0.5) mice belonged to the HFD group (Table 1).

3.2. Quantification of serum EVs in mice with atherosclerosis

Sixteen samples, excluding NCD1 and NCD6, which were not measurable owing to lack of serum, were assessed for the number of EVs sized 30–1000 nm in 100 μl PBS. This range includes exosomes and microvesicles, which have recently gained increasing attention. We serially determined the number of EVs at every 1-nm interval and averaged the number of EVs of each size in the control and HFD groups to elucidate the size distribution of EVs (Fig. 3). First, the NCD group displayed several peaks; however, the HFD group displayed a single peak pattern. The averagenumber of EVs was greater in the control group than in the HFD group in most areas (Fig. 3); however, the averagenumber of EVs sized 34.5–64.5 nm, 146.5–162.5 nm, 509.5–523.5 nm, 592.5–613.5 nm, and 941.5–999.5 nm was greater in the HFD group than in the control group (Fig. 3). The largest differentiation of average number of EVs was detected at 148.5 ˜ 157.5 nm in 5 areas (34.5–64.5 nm, 146.5–162.5 nm, 509.5–523.5 nm, 592.5–613.5 nm, and 941.5–999.5 nm). However, it was not significant, statistically ($p > 0.05$). The average number of EVs in the control group and HFD group were 43.77 x 10^9 and 20.85 $\times$ 10^9, respectively. The control group exhibited more number of EVs ($p < 0.001$). The average number of EVs in the range of 30˜100 nm was 1.29 x $10^9$and 0.11 $\times$ 10^9 for the control and HFD group, respectively. The control group exhibited a higher number of EVs than HFD group($p = 0.062$). The averagenumber EVs in the range of 100.5˜999.5 nm was 42.50 x $10^9$and 20.73 $\times$ 10^9 for the control and HFD group, respectively. The control group exhibited a higher number of EVs than HFD group ($p < 0.001$).

Among the HFD groups, the Ats was under the 0.5 score for HFD1, HFD3, HFD6, HFD8, HFD9, HFD10, and HFD12, thus constituting the low Ats group, while HFD2, HFD4, HFD5, HFD7, and HFD11 constituted the high Ats group. Furthermore, the distribution of EVs was compared. The averaged number of EVs sized 34.5–47.5 nm, 65.5–76.5 nm, 136.5–152.5 nm, 202.5–256.5 nm, 312.5–568.5 nm, 596.5–620.5 nm, and 640.5–730.5 nm was greater in the high Ats group than in the low Ats group (Fig. 4). The number of EVs in the high Ats group(1.43×10^9) was higher than that in the low Ats group (0.7×10^9), in the range of 211.5–222.5 nm ($p = 0.033$) (Table 1).

4. Discussion

EVs are ultramicroscopic cystic structures with a bilayered membrane and are secreted from numerous cell types [1]. EVs are categorized by size, and although standards vary slightly among different studies, they are usually categorized as exosomes between 30 nm and 100 nm, microvesicles between 100 nm and 1000 nm, and apoptotic bodies over 1000 nm [4,7]. Apoptotic bodies have been extensively studied in the past, and studies on exosomes and microvesicles have

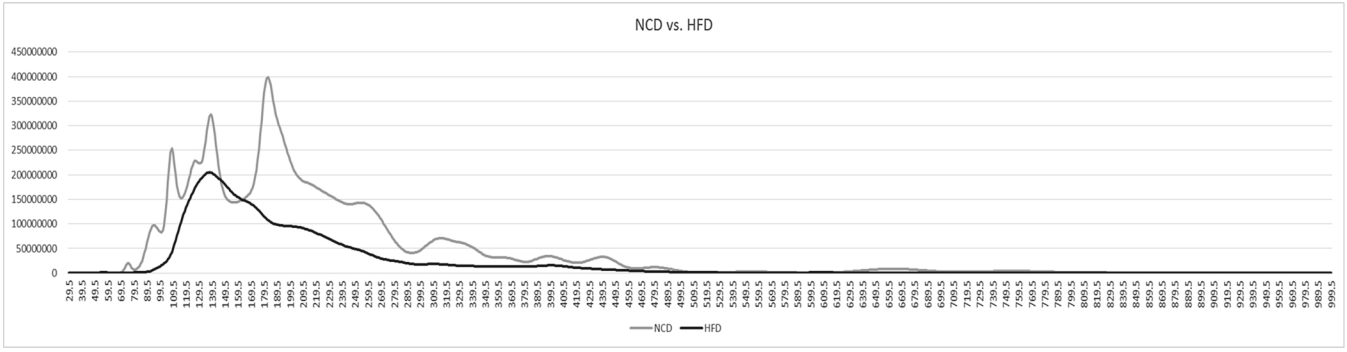

Fig. 3. Distribution of EVs by size at NCD group and HFD group by NTA. The number of EVs was measured at each 1 nm intervals between 30 nm–1000 nm. EVs, extraceullar vesicles; NTA, nanoparticle tracking analysis; NCD, normal chewing diet; HFD, high fat diet.

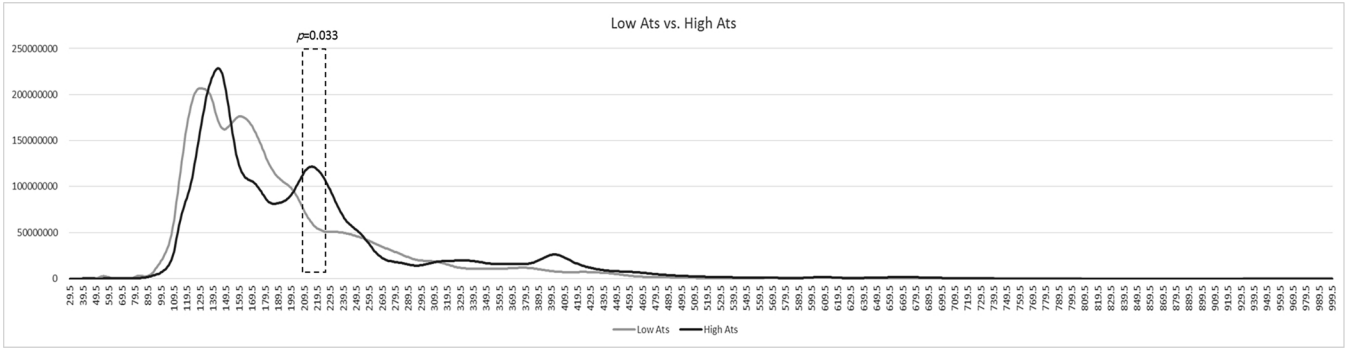

Fig. 4. Distribution of EVs by size at high Ats group and low Ats group by NTA. The number of EVs was measured at each 1 nm intervals between 30 nm–1000 nm. The area between 211.5 ~ 222.5 nm shows higher number of EVs in high Ats group than low Ats group (p = 0.033).
EVs, extraceullar vesicles; NTA, nanoparticle tracking analysis; Ats, atherosclerotic score

recently received increasing attention. EVs are particularly popular in studies on diseases as they are involved in intercellular communication, and studies are currently attempting to identify the potential for target-specific treatment of diseases or early diagnosis of diseases, as EVs are.

EVs have been actively assessed in atherosclerosis. Perrotta et al. reported that microvesicular bodies, which are exosomal precursors, are more in number in atherosclerotic tissues than in control tissues [5]. Niu et al. reported that EVs of macrophage origin display enhanced adhesion and migration among vascular smooth cells [4]. Several other studies have also reported the association between atherosclerosis and EVs [8].

This study focused on quantitative analysis of EVs. Using NTA, we enumerated EVs sized 30–1000 nm, including the recently reported exosomes and microvesicles in each 1 nm sized of EVs [9]. All samples were cleared of debris and assessed in 100 μl serum units. Interestingly, in most areas, average measurements of the control group were greater in number than those of the HFD group. And the number of EVs in the high Ats group (1.43×10^9) was higher than that in the low Ats group (0.7×10^9), in the range of 211.5–222.5 nm ($p = 0.033$). Our result suggests that these EVs sized 211.5–222.5 nm are associated with the Ats.

Atherosclerosis causes critical diseases, and it can induce fatal organ failure. Prevention therapy is required before the onset of cardiac rupture, wherein, the evaluation of atherosclerosis is necessary. Although this study has several limitations (as discussed below), it provides essential information for treating atherosclerosis patients. Further evaluation is essential on a larger scale or with human samples.

There are several limitations of this study. The aorta of mice are thin (almost 1~2 mm in diameter) and contains large amounts of perivascular fatty tissue, which presents challenges during freezing of tissue specimens and Oil red O staining. We attempted to minimize tissue loss. However, this analysis warrants biological triplicates.

In conclusion, this study describes the distribution of atherosclerotic lesions in the aorta of mice (*wild-type*) fed with an HFD. As revealed using NTA, EVs sized 211.5–222.5 nm are positively associated with the Ats.

Declarations of interest

None

Author contribution

Conceptualization: Dae Hyun Song
Data curation: Seokmin Kang, Jung Wook Yang
Formal analysis: Dae Hyun Song
Investigation: Seokmin Kang, Jung Wook Yang
Methodology: JooYeonJeong, Juyeong Park
Project administration: Dae Hyun Song
Resources: Hyo Jung An
Supervision: Hyun Min Koh
Validation: Se Min Jang
Writing—original draft: Seokmin Kang, Jung Wook Yang
Writing—review & editing: Dae Hyun Song, Yoon Jung Lee

Acknowledgment

This study was supported by Lee Jung Ja Research grant of Gyeongsang National University Hospital (LJJ-GNUH-2018-003).

Appendix A. Supplementary data

Supplementary material related to this article can be found, in the online version, at doi:https://doi.org/10.1016/j.prp.2019.152574.

References

[1] E. Bielska, P.R.J. Birch, A.H. Buck, C. Abreu-Goodger, R.W. Innes, H. Jin, M.W. Pfaffl, S. Robatzek, N. Regev-Rudzki, C. Tisserant, S. Wang, A. Weiberg, Highlights of the mini-symposium on extracellular vesicles in inter-organismal communication, held in Munich, Germany, August 2018, J. Extracell. Vesicles 8 (2019) 1590116.

[2] A. Gaceb, M.C. Martinez, R. Andriantsitohaina, Extracellular vesicles: new players in cardiovascular diseases, Int. J. Biochem. Cell Biol. 50 (2014) 24–28.

[3] R. Kojima, D. Bojar, G. Rizzi, G.C. Hamri, M.D. El-Baba, P. Saxena, S. Auslander, K.R. Tan, M. Fussenegger, Designer exosomes produced by implanted cells intracerebrally deliver therapeutic cargo for Parkinson's disease treatment, Nat. Commun. 9 (2018) 1305.

[4] C. Niu, X. Wang, M. Zhao, T. Cai, P. Liu, J. Li, B. Willard, L. Zu, E. Zhou, Y. Li, B. Pan, F. Yang, L. Zheng, Macrophage foam cell-derived extracellular vesicles promote vascular smooth muscle cell migration and adhesion, J. Am. Heart Assoc. 5 (2016).

[5] I. Perrotta, S. Aquila, Exosomes in human atherosclerosis: an ultrastructural analysis study, Ultrastruct. Pathol. 40 (2016) 101–106.

[6] R. Ross, Cell biology of atherosclerosis, Annu. Rev. Physiol. 57 (1995) 791–804.

[7] B.W. Sodar, A. Kittel, K. Paloczi, K.V. Vukman, X. Osteikoetxea, K. Szabo-Taylor, A. Nemeth, B. Sperlagh, T. Baranyai, Z. Giricz, Z. Wiener, L. Turiak, L. Drahos, E. Pallinger, K. Vekey, P. Ferdinandy, A. Falus, E.I. Buzas, Low-density lipoprotein mimics blood plasma-derived exosomes and microvesicles during isolation and detection, Sci. Rep. 6 (2016) 24316.

[8] S.A. Su, Y. Xie, Z. Fu, Y. Wang, J.A. Wang, M. Xiang, Emerging role of exosome-mediated intercellular communication in vascular remodeling, Oncotarget 8 (2017) 25700–25712.

[9] R. Szatanek, M. Baj-Krzyworzeka, J. Zimoch, M. Lekka, M. Siedlar, J. Baran, The methods of choice for extracellular vesicles (EVs) characterization, Int. J. Mol. Sci. 18 (2017).

[10] C. Thery, S. Amigorena, G. Raposo, A. Clayton, Isolation and characterization of exosomes from cell culture supernatants and biological fluids, Curr. Protoc. Cell Biol. (2006) Chapter 3 Unit 3 22.

[11] T. Thomou, M.A. Mori, J.M. Dreyfuss, M. Konishi, M. Sakaguchi, C. Wolfrum, T.N. Rao, J.N. Winnay, R. Garcia-Martin, S.K. Grinspoon, P. Gorden, C.R. Kahn, Adipose-derived circulating miRNAs regulate gene expression in other tissues, Nature 542 (2017) 450–455.

[12] M. Yin, X. Loyer, C.M. Boulanger, Extracellular vesicles as new pharmacological targets to treat atherosclerosis, Eur. J. Pharmacol. 763 (2015) 90–103.